

ICINCO 2007

FOURTH INTERNATIONAL CONFERENCE ON
INFORMATICS IN CONTROL, AUTOMATION AND ROBOTICS

Proceedings

Robotics and Automation - Vol. 2

ANGERS, FRANCE · MAY 9-12, 2007

ORGANIZED BY



IN COOPERATION WITH



CO-SPONSORED BY



ICINCO 2007

Proceedings of the
Fourth International Conference on
Informatics in Control, Automation and Robotics

Volume RA-2

Angers, France

May 9 – 12, 2007

Co-organized by
**INSTICC – Institute for Systems and Technologies of Information, Control
and Communication**
and
University of Angers

Co-sponsored by
IFAC - International Federation of Automatic Control
**GDR MACS - Groupe de Recherche “Modélisation, Analyse et Conduite
des Systèmes dynamiques**
CNRS - Centre National de la Recherche Scientifique
and
**EEA – Club des Enseignants en Electronique, Electrotechnique
et Automatique**

In Cooperation with
AAAI – Association for the Advancement of Artificial Intelligence

Copyright © 2007 INSTICC – Institute for Systems and Technologies of
Information, Control and Communication
All rights reserved

Edited by Janan Zaytoon, Jean-Louis Ferrier, Juan Andrade Cetto and Joaquim Filipe

Printed in Portugal

ISBN: 978-972-8865-83-2

Depósito Legal: 257879/07

<http://www.icinco.org>

secretariat@icinco.org

ESTIMATION OF CAMERA 3D-POSITION TO MINIMIZE OCCLUSIONS

Pablo Gil, Fernando Torres

*Department of Physics, Systems Engineering and Signal Theory, University of Alicante, Crta. San Vicente s/n
Alicante, Spain, Pablo.Gil@ua.es, ftorres@dfists.ua.es*

Oscar Reinoso

*Department of Industrial Systems Engineering, Miguel Hernandez University
Elche, Spain o.reinoso@umh.es*

Keywords: Occlusions, Camera viewpoint, Camera pose, Segmentation.

Abstract: Occlusions are almost always seen as undesirable singularities that pose difficult challenges to recognition processes of objects which have to be manipulated by a robot. Often, the occlusions are perceived because the viewpoint with which a scene is observed is not adapted. In this paper, a strategy to determine the location, orientation and position, more suitable so that a camera has the best viewpoint to capture a scene composed by several objects is presented. The estimation for the best location of the camera is based on minimizing the zones of occlusion by the analysis of a virtual image sequence in which is represented the virtual projection of the objects. These virtual projections represent the images as if they were captured by a camera with different viewpoints without moving it.

1 INTRODUCTION

In Computer vision, one of the critical problems for object recognition is that the recognition methods should be able to handle partial occlusion of objects. The spatial distribution of structural features of an object is the most important information that an object represents. Recognition partially occluded objects have been a formidable problem in recognition processes. In recent years, several object recognition methods have been proposed to recognize occluded objects. Some of them are based on statistical models (Chan, 2002)(Ying, 2000), on graph models (Boshra, 2000)(El-Sonbaty, 2003) or based on a mix (Park, 2003). Also it is important to emphasize others studies which are based on the eigenspace analysis of images taken in the same environment. Thus an object model is built as a vector in a low dimensional eigenspace, and this way objects are recognized by comparing the model with image vectors.

The ability to recognize an object in an image is limited if it is impossible to see all the surface of the object. Not only self-occlusion are present in opaque objects since we are not able to see the back of the object, but also other objects may occlude

some portion of the object that we wish to recognize and that it would otherwise be visible. In our approach, we look to change the location of the camera which observes the objects in order to improve the viewpoint and reduce the occluded portion of them. Other works, such as (Silva, 2001) show in their studies the importance of the occlusions for motion detection and the relation between the observable occlusions and a camera motion. Also, in recent years, some works have shown how compute 3D-structure from camera motion using the matching process among image plane projections by employing the Shift Invariant Feature Transform, SIFT features (Fiala, 2005)(Ohayon, 2006).

This paper is organized as follows: The mathematical principles to understand the camera motion are described in Section II. Section III shows the relationship between the 3D-position of a camera and the position of an object projected in an image captured by it. In Section IV, a strategy to determine zones of occlusion between objects from information of an image is presented and experimental results are shown. Section V describes the process to evaluate and verify the best viewpoint which minimizes the zone of occlusion detected in the image. Finally, the validity of the method

proposed is confirmed with a camera at the end of an arm robot.

2 CAMERA MOTION AS RIGID BODY

As starting point a camera moving in front of several objects in a scene can be considered. The camera and objects are modelled as rigid objects. Therefore, each motion can be specified as the motion of one point on the object in respect to another on the camera, the reason being because the distance between any two points which belong to the same object does not change when this object is moved. Consequently, it is not necessary to specify the trajectory of every point on the object in respect to the camera. So, the inertial central moment is the only point we have to consider on the objects, and the optical center is the only point we have to consider on the camera.

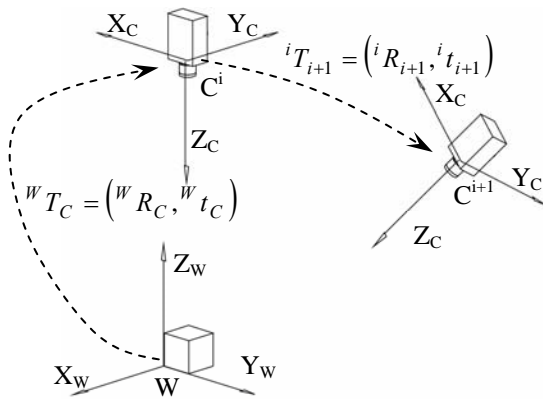


Figure 1: Camera movement relative to world reference frame W .

Thus, if C^0 are the coordinates of the camera C in the time $i=0$, and C^i , the coordinates of the same point on Camera in the time $i>0$, the geometric transformation which is experimented by camera, is given by:

$$T: R^3 \rightarrow R^3 / C^0 \rightarrow T \cdot C^i \quad (1)$$

If the camera motion is represented in relation to a world reference frame W , and this one is considered fixed, without movement, then the camera motion C is defined by rotational and translational movements which are relative to W in the Euclidean Space. These Euclidean transformations are denoted by wR_C and wt_C , respectively. So, any point which is

relative to W can be posed relative to C with this equation.

$$P_w = {}^wT_C \cdot P_C = {}^wR_C \cdot P_C + {}^wt_C \quad (2)$$

where wT_C denotes an Euclidean transformation that represents rotation and translation movements of W in relation to C , and P_C is the point relative to C . To this end, the equation 2, is converted to homogeneous representation, appending a '1' to the coordinates of P_C , that is $P_C = (P_C, 1)^T \in R^4$. Thus a matrix form is used to rewrite it since a linear form is more suitable to operate.

$$P_w = \begin{bmatrix} {}^wR_C & {}^wt_C \\ 0 & 1 \end{bmatrix} \cdot P_C \quad (3)$$

3 A GEOMETRIC MODEL OF IMAGE FORMATION

In this section, the mathematical model of the image formation process is introduced (Hartley, 2000)(Gruen, 2001). The pinhole camera is chosen as the ideal model to define computer vision processes, and to specify the image formation process, particularly. This process can be described as a set of transformation of coordinates between the camera frame and the world frame (Section 2) and transformations of projection of 3-D object coordinates relative to camera onto 2-D image coordinates. The transformations which determine the movement of a rigid body are defined in Euclidean space, and the transformations which determine the projection onto the image plane are defined in the Projection space.

The pinhole camera model assumes that each 3D-point on an object is projected onto a camera sensor through a point called the optical center. The origin of the reference frame C is at this optical center and the coordinates of a 3D-point relative to C are denoted by $P_C(X, Y, Z)$. In addition, the coordinates of the same point on the image plane which is projected through the camera sensor are $p_I(x, y)$, where the reference frame image is called I . The origin of the reference frame I is the principal point o which is the intersection point of the optical axis with the image plane, and the parameter f defines the distance of image plane from the optical center.

With reference to the pinhole camera model, the transformation between the reference frames C and I can be represented in homogeneous coordinates and matrices, as follows:

$$Z \begin{bmatrix} x \\ y \\ 1 \end{bmatrix} = \begin{bmatrix} fX \\ fY \\ Z \end{bmatrix} = \begin{bmatrix} f & 0 & 0 & 0 \\ 0 & f & 0 & 0 \\ 0 & 0 & 1 & 0 \end{bmatrix} \cdot \begin{bmatrix} X \\ Y \\ Z \\ 1 \end{bmatrix} \quad (4)$$

where Z is the depth of the object and f is the focal length.

If the equation is decomposed in two matrices, K_f y Π_0 , where the first matrix is called focal matrix, and the second matrix is often referred to as canonical projection matrix, the ideal model can be described as

$$p_I = K_f \cdot \Pi_0 \cdot P_C \quad (5)$$

However, in practice, the projection transformation between C and I , is very much complex. The matrix K_f depends on others parameters as the size of the pixels, the form of the pixels, etc. Therefore, a method to make the geometric formation image more suitable, is needed. The practice model has to consider (according to (Ma, 2004)):

- The size of pixels. The reason is because the size of the sensor is different to the size of the image. Therefore, the scaling factors (s_x, s_y) must be considered. A point on image plane $p_I(x, y)$ in terms of mm is projected as a point on image $p(u, v)$ in terms of pixels.
- The pixels are not square and do not have orthogonal axis. Therefore, a factor called skew, s_θ , can be used to define the angle between the image axes.
- In addition, the origin of image plane does not coincide with the intersection of the optical axis and the image plane. There is a translational movement between the geometric center on image and the principal point. For this reason the principal point is computed by a calibration process (Zhang, 1999).

If the ideal projection model, pinhole model camera, is modified with these parameters to adapt it to the formation image process and a CCD camera is used, the Equation 5 can be rewritten in the following way:

$$p = K_s \cdot K_f \cdot \Pi_0 \cdot P_C = K \cdot \Pi_0 \cdot P_C \quad (6)$$

where the triangular matrix, $K=K_s \cdot K_f$, is known as the calibration matrix or intrinsic parameters matrix and its general form is:

$$K = \begin{bmatrix} fs_x & fs_\theta & o_x \\ 0 & fs_y & o_y \\ 0 & 0 & 1 \end{bmatrix} \quad (7)$$

A calibrated camera with a checkboard pattern has been used in this work. The values for K are: $f=21\text{mm}$, $s_x=96.6\text{pixels/mm}$, $s_y=89.3\text{pixels/mm}$, $s_\theta=0$, $o_x=331\text{pixels}$ y $o_y=240\text{ pixels}$.

4 MINIMIZING OCCLUSIONS

The aim of the work presented in this paper is to minimize the zones of occlusions of an object in a scene in which several objects are present. This object has part of its surface occluded by other objects. A camera moving in front of the scene is used to obtain a viewpoint that reduces the occlusion zone of the object desired. Thus, the visibility of the object partially occluded will be improved. This means that more surface of the object desired can be captured by camera.

In the time 0, the initial camera position is given by C^0 . On the other hand C^i where $i > 0$ represents the camera position at every moment of time. In addition, the camera position which offers the best viewpoint is represented by C^{i*} . This camera position is the position which minimizes the occlusion zone of the desired object, and which maximizes its visible surface.

In order to avoid modifying the intrinsic parameters matrix of the camera, the space of movements for the camera has been limited. Thus the movement of the camera has been planned like a point which is moved on a hemispheric surface. This way the objects in the scene are located in the center of the hemisphere and the camera can only be located in positions C^i which maintain the same distance to the objects that shown by C^0 . Therefore, the distance between camera and objects does not change. This distance is determined by the ratio of the hemisphere, r , which limits the space search of the possible position for the camera. As a result, the camera does not need to be recalibrated because it is not necessary to obtain a new focal length. A study about the suitable movement of a camera into regions sphere is shown in (Wunsch, 1997).

Each camera position is determined by two parameters: length and latitude. Each position, $P_C(X, Y, Z)$ is defined by the displacements in length relative to the initial position, C^0 , which is determined by the angle $\theta \in [0, 2\pi]$ and by the displacements in latitude which is determined by the angle $\varphi \in [0, \pi/2]$. This way, it is possible to define any possible position which can be adopted by the

camera in the hemispheric search space. The greatest number of positions that the camera can adopt is defined by $\forall C^i / i=0..\pi^2$. This defines the complete space of camera position. Displacements of 1 degree for length and latitude have been respectively taken.

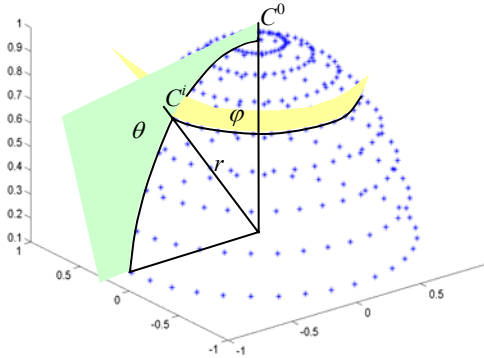


Figure 2: Space of movements for the camera.

The value for each iteration, determined by length and latitude angles, can be modified to increase or to reduce the search space of camera positions. These parameters are chosen depending on the velocity of computation for the analysis of camera positions, and the precision to compute the best camera position for a good viewpoint.

To obtain the best camera position, two parameters have been evaluated: distances and areas. If the zones of occlusion detected in the image must be diminished, the objects in image space must be separated as far as possible.

$$C^{i*} \text{ is } C^i / \max\{d(o_k, o_{k+1})\} \text{ in image } i \quad (8)$$

Therefore, the first evaluated parameter is the distance between objects. The minimum distance between two objects represented in image space, o_k and o_{k+1} is chosen as the minimum distance between the points of each object. It is described as:

$$d(o_k, o_{k+1}) = \min\{d(\bar{p}_k, \bar{p}_{k+1})\} \quad (9)$$

where $\bar{p}_k = (p_{k1}, \dots, p_{kn})$ is the vector of points which represent the object o_k in space image, and where each point of object $p_{ki} = (u_{ki}, v_{ki}) \in R^2$.

The distance is computed as the length of the line segment between them. Two kinds of distance are used: the distance between the centroid of objects and the distance between the points of edges, which represent the object boundaries. In three-space, the distance does not change because the objects are not in movement. Nevertheless, in image space, the distance changes because the position of

an object in relation to another depends on the viewpoint of the camera which is used to capture the image. A comparison of both distance parameters is shown in Figure 3. The distances computed among edge points decreases and converge to zero when an object occludes another. Although, if the distance is computed from the centroids of the segmented region, it can be unstable because when an object occludes another, the first modifies the centroid of the second. The second parameter is the area of each object. This is the visible surface of each object. For the study of the object areas, two cases can be considered.

First case: The viewpoint of camera is not changed and only the location of an object is modified until another is occluded (the movement is in the same orthogonal plane relative to the camera). So, the visible surface of the object occluded has been decreased and the rest of the objects maintain the same area visible. This is shown in Figure 4.

Second case: The viewpoint of the camera is changed and a new perspective is made in the image captured by it. Thus, the area of each object is changed (see Figure 5). But also, when several poses of camera compute a measure of distance, this fact indicates that occlusions are not present.

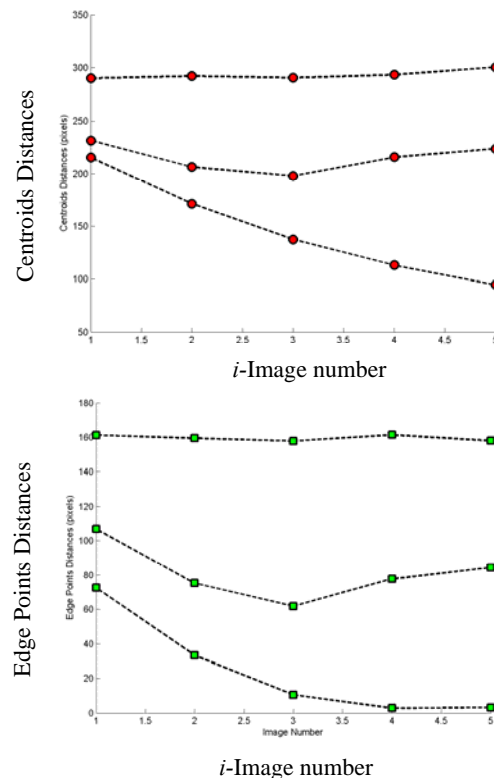


Figure 3: Distances between objects evaluated for the images shown in Figure 4.

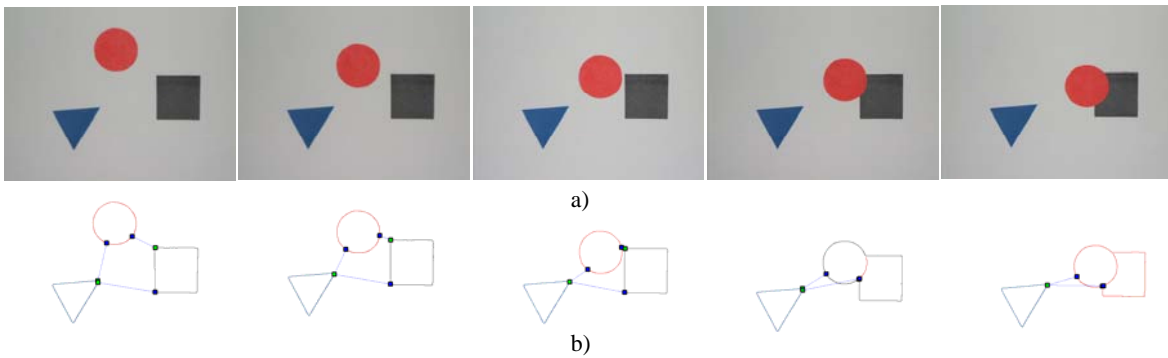


Figure 4: Distances computed among synthetic objects in real images. a) Image sequence with movement of an object. b) Objects segmented from colour and edges, and distances computed from points of edges.

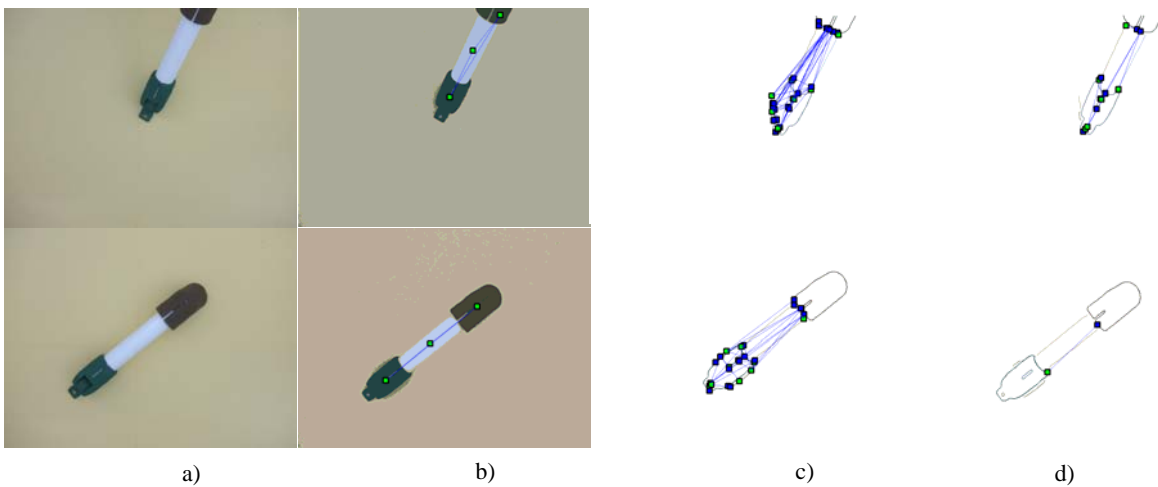


Figure 5: Distances computed among real objects in images. a) An assembly of several objects. b) Distance considering center of gravity. c) Distance considering points of edges. d) Distance considering only optimized points of edges.

Thus, the measure of area of each object must be evaluated and the best pose of camera is one in which the perspective in the image maximizes the sum of areas of each object.

Figure 5b shows the experimental results of applying a colour segmentation process to obtain object regions and, in this way, computing areas (Gil, 2006). In addition, only the segmented regions with a number of pixels major than 5% of pixels in image are taken as objects except the background which is the region with the major number of pixels. For these regions, not only the centroids are computed but also the distances between them. For this experiment, the segmentation process detects 6 regions, however only 3 regions are marked as objects from 3 automatic thresholds by each colour component.

Figure 5c shows the edge segmentation process of colour regions computed in Figure 5b and the distance computed between points of edges belongs

to different objects. Finally, Figure 5d shows the distance computed between objects when only optimized edges are considered. The optimized edges are the detected edges which have a number of points major than the standard deviation. The standard deviation determines the measure of variability of the number points which determine an edge from its mean. For this experiment, the detected edges have been 9 and 13 respectively, and the optimized edges 3 and 5 respectively. These edges are approached by segments.

Table 1: Distances between objects computed from the two real views shown in Figure 5 using centroids and points of edge.

Objects	View 1	View 2
d(1,2)	208,129 (129,448)	252,621 (145)
d(1,3)	112,397 (6,403)	123,465 (4,123)
d(2,3)	96,714 (14,422)	129,176 (9,055)

Table 1 shows how the distances computed from centroids are increased if the camera makes the movement shown in Figure 5. Nevertheless, the distances computed from the points of edges can be increased slowly if the real distance between objects is closely near to zero. This fact is due to small instabilities when two real images with different perspective of a same scene are used to obtain segments of boundary. Then, not always the same points are detected in both images.

Although, this is not a problem because the computed distances are always calculated from edges back-projected in virtual images. Therefore, the same points of edges appear in all the virtual images, and only their positions in image are changed.

5 POSE CAMERA TO MINIMIZE OCCLUSION

RGB-colour images with size 640x480 have been used in this work. The steps to explain this work are detailed as follows.

In the first step, an initial image is captured from the initial camera pose, C^i . The 2D-points into initial image are obtained from a colour and edges segmentation process (Gil, 2006). An example of this process has been shown in Figure 5. Next, the distances between objects and its areas are computed for this initial image. Afterwards, for this first image, Equation 3 give the transformation between world coordinates and camera coordinates to obtain 3D-points relative to C^i . Also, the projective matrix, Π , maps 3D-points, relative to C^i , to image points $p(u, v)$ according to Equation 6. Given the points in an image, a set of 3D-points in space that map these points can be determined by means of back-projection of 2D-points. That is:

$$P = \Pi^+ p^i = (K \cdot \Pi_0 \cdot {}^W T_{C^i})^+ p^i, / i = 1..n \quad (10)$$

where n is number of position for the camera and the pseudo-inverse of Π is the matrix $\Pi^+ = \Pi^T (\Pi \Pi^T)^{-1}$ which verify that $\Pi \Pi^+ = I$. Equation 10 can be rewritten as a homography matrix, so that:

$$P = H_i^{-1} p^i \quad (11)$$

When the 3D-points are known, the second step consists of computing the projections of the 3D-points which belong to objects from space of camera poses (see Figure 2). This means that the 3D-points are mapped onto each virtual image for each camera

pose, as shown in Figure 6. Thus, virtual 2D-points are computed. It is given by:

$$p^{i+1} = H_{i+1} \cdot P = H_{i+1} H_i^{-1} p^i \quad (12)$$

These virtual points determine the regions and edges of objects in virtual images. Finally, the distances between objects and areas of each object are computed in each virtual image (Section 4).

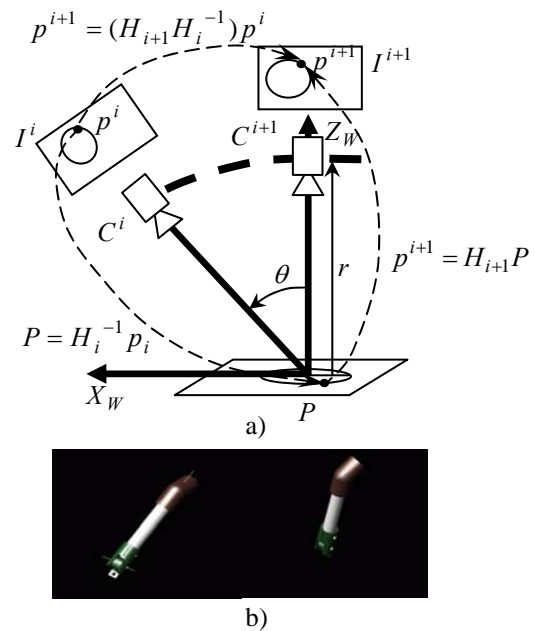


Figure 6: a) Mapping points onto virtual images according to camera movement. A displacement in length has been mapped. b) CAD-Model of assembly used in Figure 5.

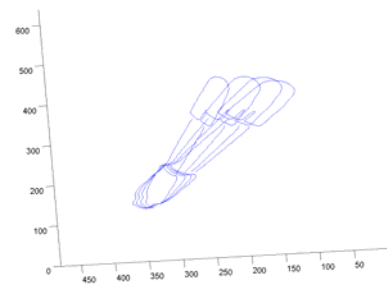


Figure 7: Back-projections onto virtual images from camera movements.

Therefore, a set of ${}^M T_{C^i}$ are evaluated as shown in Figure 2. And the back-projection for each ${}^M T_{C^i}$ is computed (see Figure 7). Concluding, the best pose of the camera is determined by the transformation which maximizes the distances and the areas in the space of virtual images. This transformation is given by the perspective matrix,

and it determines what transformations ${}^W R_{C_i}$ and ${}^W T_{C_i}$ are more suitable. Afterwards, a robot PA-10 from Mitsubishi, with 7 degrees of freedom, moves the camera mounted at its end to more suitable computed pose.

6 CONCLUSIONS

The presented work provides an input to an object recognition process. Thus, a method based on extraction of characteristics in image, which is based on the evaluation of the distances among these characteristics, is used to determine when an occlusion can appear. In addition, the method evaluates the camera pose of a virtual way from the back-projections of the characteristics detected in a real image. The back-projections determine how the characteristics are projected in virtual images defined by different camera poses without the necessity of camera is really moved. The experimental results have shown that the proposed estimation can successfully be used to determine the camera pose that is not too sensitive to occlusions. However, the approach proposed does not provide an optimal solution. This could be solved by applying visual control techniques which are currently under investigation.

Our future work will extend this approach to incorporate visual servoing in camera pose, allowing for a robust positioning camera. A visual servoing system with a configuration ‘eye-in-hand’ can be used to evaluate each camera pose (Pomares, 2006). Thus, the errors can be decreased and the trajectory can be changed during the movement. In addition, the information provided from a model CAD of the objects (see Figure 6b) can be used to verify camera poses in which it is located.

ACKNOWLEDGEMENTS

This work was funded by the Spanish MICYT project “Diseño, implementación y experimentación de escenarios de manipulación inteligentes para aplicaciones de ensamblado y desensamblado automático (DPI2005- 06222)”.

REFERENCES

- Boshra, M., Ismail, M.A., 2000. Recognition of occluded polyhedra from range images. *Pattern Recognition*. Vol. 3, No. 8, 1351-1367.
- Chan, C.J., Chen S.Y., 2002. Recognition Partially Occluded Objects Using Markov Model. *Int. J. Pattern Recognition and Artificial Intelligence*. Vol. 16, No. 2, 161-191.
- El-Sonbaty, Y., Ismael, M.A., 2003. Matching Occluded Objects Invariant to Rotations, Translations, Reflections, and Scale Changes. *Lecture Notes in Computer Science*. Vol. 2749, 836-843.
- Fiala, M., 2005. Structure From Motion Using SIFT Features and PH Transform with Panoramic Imagery. *Second Canadian Conference on Computer and Robot Vision*. Victoria, BC, Canada.
- Gil, P., Torres, F., Ortiz, F.G., Reinoso, O., 2006. Detection of partial occlusions of assembled components to simplify the disassembly tasks. *International Journal of Advanced Manufacturing Technology*. No. 30, 530-539.
- Gruen, A., Huang, T.S., 2001. *Springer Series in Information Sciences. Calibration and Orientation of Cameras in Computer Vision*. Springer-Verlag Berlin Heidelberg New York.
- Hartley, R., Zisserman, A., 2000. *Multiple View Geometry in Computer Vision*. Cambridge University Press.
- Ma, Y., Soato S., Kosecka J., Shankar S., 2004. *An Invitation to 3-D Vision from Images to Geometric Models*. Springer-Verlag, New York Berlin Heidelberg.
- Ohba, K., Sato, Y., Ikeuchi, K., 2000. Appearance-based visual learning and object recognition with illumination invariance. *Machine Vision and Applications* 12, 189-196.
- Ohayon, S., Rivlin, E., 2006. Robust 3D Head Tracking Using Camera Pose Estimation. *18th International Conference on Pattern Recognition*. Hong Kong.
- Park, B.G., Lee K.Y., Lee S.U., Lee J.H., 2003. Recognition of partially occluded objects using probabilistic ARG (attributed relational graph)-based matching. *Computer Vision and Image Understanding* 90, 217-241.
- Pomares, J., Gil, P., Garcia, G.J., Torres, F., 2006. Visual-force control and structured Light fusion improve object discontinuities recognition. *11th IEEE International Conference on Emerging Technologies and Factory Automation*. Praga.
- Silva, C., Victor, J.S., 2001. Motion from Occlusions. *Robotics and Autonomous Systems* 35, 153-162.
- Ying, Z., Castañon, D., 2000. Partially Occluded Object Recognition Using Statical Models. *Int. J. Computer Vision*. Vol. 49, No. 1, 57-78.
- Wunsch, P., Winkler S., Hirzinger, G., 1997. Real-Time Pose Estimation of 3-D Objects from Camera Images Using Neural Networks. *IEEE International Conference on Robotics and Automation*. Albuquerque, New Mexico, USA.
- Zhang, Z., 2000. A flexible new technique for camera calibration. *IEEE Transactions on Pattern Analysis and Machine Intelligence*, Vol 22. No. 11, 1330-1334.

AUTHOR INDEX

Abba, G.....	333	Colle, E.....	201
Achour, K.....	195	Collins, J.....	492
Adán, A.....	318	Collins, T.....	492
Aldavert, D.....	292	Courboulay, V.....	270
Ali, S.....	402	Coyle, E.....	412
Alsina, P.....	39	Cret, O.....	455
Amirat, Y.....	446	Crispin, Y.....	149
Anton, F.....	131	Croulard, V.....	217
Anton, S.....	131	Crowther, W.....	504
Aoustin, Y.....	76	Crunk, S.....	229
Arámburo-Lizárraga, J.....	189	Cruz, J.....	478
Araujo, A.....	39	Dabe, F.....	65
Assad, O.....	217	David, F.....	326
Augusto, S.....	390	Delafosse, M.....	438
Babic, J.....	430	Delahoche, L.....	438
Badreddin, E.....	341, 485	Déniz, O.....	384, 418
Baglivo, L.....	11	DeSouza, G.....	286
Bayro-Corrochano, E.....	175, 183	Dias, S.....	39
Beldona, S.....	84	Díaz, C.....	19
Bellas, F.....	53	Díaz, M.....	161
Bernardi, R.....	478	Djama, Z.....	446
Bertholom, A.....	65	Domínguez, M.....	5
Bertolazzi, E.....	11	Ducard, G.....	124
Bez, H.....	169	Duník, J.....	223
Bhaskar, H.....	169	Duro, R.....	53
Bittermann, M.....	468	Elloumi, H.....	209
Blazevic, P.....	396	El-Shenawy, A.....	485
Boranguiu, T.....	131	Faíña, A.....	53
Bordier, M.....	209	Faure, A.....	402
Breen, D.....	412	Feliú, V.....	318
Budisic, M.....	430	Ferreira, A.....	390
Cadden, G.....	229	Floquet, T.....	195
Canalis, L.....	384	Gabriele, S.....	237
Capezio, F.....	252	Geering, H.....	124
Carrasco E., A.....	280	Giamberardino, P.....	237, 259
Caselli, S.....	355	Gil, P.....	311
Castrillón, M.....	384, 418	Godinho, A.....	370
Cecco, M.....	11	Godoy, E.....	217
Chaumont, R.....	110	Goerke, N.....	347
Chérif, A.....	446	Goldsmith, P.....	280
Chevallereau, C.....	76	Gomà, A.....	161
Chintoanu, M.....	455	Gonçalves, A.....	370
Ciftcioglu, O.....	468	González, E.....	318
Císcar, F.....	70	Guerra, C.....	418
Clerentin, A.....	438	Hahn, H.....	424

AUTHOR INDEX (CONT.)

Hamerlain, F.	195	Michel, N.	59
Häming, K.	275	Miori, G.	11
Hamon, L.	33	Miyoshi, T.	25, 243
Han, K.	286	Monica, F.	355
Hashimoto, H.	396	Morette, N.	45
Hashimoto, K.	498	Nagendran, A.	504
Haverinen, J.	137	Naik, S.	229
Hebbel, M.	378	Nait-Chabane, K.	201
Hess, M.	116	Ninh, K.	229
Histace, A.	270	Nisticò, W.	378
Hofer, M.	229	Noda, Y.	25, 243, 498
Homolová, J.	223	Novales, C.	45
Hoppenot, P.	201	Oboe, R.	11
Hrebień, M.	305	Ohyama, Y.	396
Ibarra M., S.	461	Ostrovsky, A.	408
Illerhues, J.	347	Otero, S.	5
Inglese, F.	33	Pecherková, P.	223
Jaulin, L.	65	Pepy, R.	98, 103
Jolly-Desodt, A.	438	Perruquetti, W.	195
Josserand, L.	45	Peters, G.	275
Kalaykov, I.	92	Petrovic, I.	430
Kawabata, K.	396	Philippe, V.	59
Kemppainen, A.	137	Pierre, E.	98, 103
Kennedy, D.	412	Pino-Mota, E.	408
Kitagawa, H.	25	Ponsa, P.	161
Kitamura, S.	25	Poza, F.	5
Kivijakola, J.	137	Puente, S.	19
Kobayashi, H.	396	Quintero M., C.	461
Korbicz, J.	305	Ramírez-Treviño, A.	189
Kowalczyk, W.	155	Ramisa, A.	292
Kozłowski, K.	155	Reggiani, M.	355
Kumar, T.	143	Reimer, M.	363
Lazea, G.	455	Reinoso, O.	311
Lefebvre, D.	110	Richard, P.	33
Legris, M.	65	Richardson, R.	143, 504
Léonard, F.	333	Ricour, M.	149
López-Mellado, E.	189	Rizzini, D.	355
Lorenzo, J.	384, 418	Romero-Soria, P.	408
Maciá, F.	70	Röning, J.	137
Mahuampy, S.	59	Rosa, J.	461
Maïzi, N.	209	Rüdiger, J.	341
Mántaras, R.	292	Ryan, C.	492
Mariño, P.	5	Sánchez, L.	318
Martini, A.	333	Sariyildiz, I.	468
Ménard, M.	270	Saska, M.	116